Proteomic Evaluation and Validation of Cathepsin D Regulated Proteins in Macrophages Exposed to *Streptococcus pneumoniae*

Martin A. Bewley‡, Trong K. Pham§, Helen M. Marriott‡, Josselin Noirel§, Hseuh-Ping Chu‖, Saw Y. Ow§, Alexey G. Ryazanov‖, Robert C. Read‡,‡‡ Moira K. B. Whyte‡‡, Benny Chain¶, Phillip C. Wright§, and David H. Dockrell‡‡‡**

Macrophages are central effectors of innate immune responses to bacteria. We have investigated how activation of the abundant macrophage lysosomal protease, cathepsin D, regulates the macrophage proteome during killing of *Streptococcus pneumoniae*. Using the cathepsin D inhibitor pepstatin A, we demonstrate that cathepsin D differentially regulates multiple targets out of 679 proteins identified and quantified by eight-plex isobaric tag for relative and absolute quantitation. Our statistical analysis identified 18 differentially expressed proteins that passed all paired *t*-tests ($\alpha = 0.05$). This dataset was enriched for proteins regulating the mitochondrial pathway of apoptosis or inhibiting competing death programs. Five proteins were selected for further analysis. Western blotting, followed by pharmacological inhibition or genetic manipulation of cathepsin D, verified cathepsin D-dependent regulation of these proteins, after exposure to *S. pneumoniae*. Superoxide dismutase-2 up-regulation was temporally related to increased reactive oxygen species generation. Gelsolin, a known regulator of mitochondrial outer membrane permeabilization, was down-regulated in association with cytochrome *c* release from mitochondria. Eukaryotic elongation factor (eEF2), a regulator of protein translation, was also down-regulated by cathepsin D. Using absence of the negative regulator of eEF2, eEF2 kinase, we confirm that eEF2 function is required to maintain expression of the anti-apoptotic protein Mcl-1, delaying macrophage apoptosis and confirm using a murine model that maintaining eEF2 function is associated with impaired macrophage apoptosis-associated killing of *Streptococcus pneumoniae*. These findings demonstrate that cathepsin D regulates multiple proteins controlling the mitochondrial pathway of macrophage apoptosis or competing death processes, facilitating intracellular bacterial killing. ***Molecular & Cellular Proteomics 10: 10.1074/mcp.M111.008193, 1–14, 2011.***

Tissue macrophages are central effectors of innate immunity against pathogenic micro-organisms, complementing the action of other components of the innate immune response (1). Transcriptomic and proteomic analysis confirms the broad range of genes that are activated in macrophages by micro-organisms (2–5). Phagocytosis and intracellular killing in phagolysosomes activates multiple signal transduction pathways whose concerted activity leads to a regulated host response to pathogens (6).

A central component of the macrophages capacity to handle ingested bacteria is its highly developed phagolysosomal system, which distinguishes the cell from other phagocytes (7, 8). Phagosomes fuse with lysosomes containing proteases, of which cathepsin D is one of the most abundant in macrophages (9). Cathepsin D expression in macrophages is highly differentiation dependent (10, 11). Cathepsin D is an aspartic protease, which possesses activity against a broad range of substrates (12). It plays a role in neurologic development, immune homeostasis, apoptosis initiation, and tumor development (12). Although cathepsin D was formerly believed to act principally within the low pH environment of the lysosome, it has become apparent that it can have residual activity outside the lysosomal compartment (13). The role of cathepsin D in host defense is currently unclear, although it has been documented to cleave the cholesterol-dependent cytolysin listerolysin produced by *Listeria monocytogenes* (14). We have recently identified a critical role for cathepsin D in the host response of macrophages against *Streptococcus pneumoniae* (15). Cathepsin D activation was observed in macrophages following ingestion of *S. pneumoniae* into phagolysosomes and played a role in the induction of macrophage apoptosis, which contributed to microbial killing. Cathepsin D

From the ‡Medical School ‡‡Sheffield Teaching Hospitals and §ChELSI Institute, Department of Chemical and Processing Engineering, University of Sheffield, Sheffield, UK.; ¶Division of Infection and Immunity, University College London, London, UK; ‖Department of Pharmacology University of Medicine and Dentistry of New Jersey-Robert Wood Johnson Medical School, New Jersey, USA

Received January 26, 2011, and in revised form, April 1, 2011
⌘ *Author's Choice*—Final version full access.
Published, MCP Papers in Press, April 7, 2011, DOI 10.1074/mcp.M111.008193

is well positioned to transduce signals from the phagolysosome during the intracellular killing of bacteria, but it is unclear how such an effect might be mediated.

In the current study, we applied an isobaric tag for relative and absolute quantitation (iTRAQ)[1] proteomic approach to identify proteins that were differentially expressed in macrophages during infection with *S. pneumoniae* (pneumococci) in the presence of an aspartic protease inhibitor, pepstatin A, as compared with vehicle control. We identified a number of differentially expressed proteins and confirmed their differential expression, after both pharmacological inhibition and genetic manipulation of cathepsin D, relating these to recognized features of pneumococcal infection in macrophages. We demonstrate that a number of these proteins regulate aspects of macrophage apoptosis, a process we have previously described as being critical to the successful control of pneumococcal infection in macrophages (16–18). In particular, we find that proteins known to regulate oxidant stress, endoplasmic reticulum (ER) stress, the expression of short-lived anti-apoptotic proteins and mitochondrial outer membrane permeabilization were differentially regulated in the presence of cathepsin D inhibition.

EXPERIMENTAL PROCEDURES

Bacteria—Type 2 *S. pneumoniae* (D39 strain, NCTC 7466) were grown in Brain Heart Infusion (BHI) media supplemented with 20% v/v fetal calf serum (FCS) until an $OD_{610\ nm}$ of 0.6 was reached. Prior to infection, thawed aliquots were opsonized in RPMI (Sigma-Aldrich) containing 10% v/v antipneumococcal immune serum (16). For mouse experiments type 1 *S. pneumoniae* (WHO reference laboratory strain SSISP; Statens Serum Institut) were handled under identical conditions but were not opsonized before instillation. Bacterial numbers were assessed by the surface viable count method after inoculation on blood agar (16).

Cells and Infection—THP-1 cells were cultured in RPMI plus 10% v/v FCS (complete media). THP-1 cells were differentiated to a macrophage phenotype by treating 0.4×10^6 cell/ml with 200 nM phorbol 12-myristate 13-acetate for 3 days, after which the phorbol 12-myristate 13-acetate was removed, and the cells left to rest for a further 5 days after which cell numbers were determined. These cells have a phenotype similar to monocyte-derived macrophages (MDM), as evidenced by nuclear to cytoplasmic ratio, concentration of mitochondria and lysosomes, cell surface markers, phagocytic capacity, cytokine generation to Toll-like receptor agonists, and susceptibility to apoptosis (19). Human MDMs were isolated from whole blood donated by healthy volunteers as previously described with informed consent as approved by the South Sheffield Regional Ethics Committee of Royal Hallamshire Hospital (Sheffield, United Kingdom) (16). After 14 days, representative wells were scraped to determine cell numbers. Murine bone-marrow derived macrophages (BMDM)s were isolated by culturing marrow from mice deficient in cathepsin D (20) or eukaryotic elongation factor 2 kinase (eEF2k) (21), or from the corresponding wild-type littermates. BMDMs were plated at 0.5×10^6 cells/ml for 14 d in Dulbecco's modified Eagles medium containing 10% FCS and 10% conditioned L929 media (17). All cell types were infected with opsonized *S. pneumoniae* at a multiplicity of infection of 10, or mock-infected (MI) as described elsewhere (16). Cells were incubated with 100 μM of the aspartic protease inhibitor pepstatin A or dimethylsulfoxide vehicle control.

SDS-PAGE and Western Immunoblotting—Whole-cell extracts and cytosolic fractions were isolated as previously described (18). Blots were incubated overnight at 4 °C with antibodies against either gelsolin (rabbit polyclonal, 1:1000; Abcam, Cambridge, MA), SOD-2 (rabbit polyclonal 1:1000; Abcam), heat shock protein (Hsp) A5/glucose-regulated protein (Grp)78/BiP (rabbit polyclonal 1:200; Abcam), S100 calcium binding protein A6/calcyclin (rabbit polyclonal 1:1000; Abcam), murine induced myeloid cell leukemia myeloid cell leukemia sequence 1 (Mcl-1), (rabbit polyclonal, 1:1000; Rockland, Rockland ME), cytochrome *c* (mouse monoclonal, 1:1000; BD Biosciences), cathepsin D (goat polyclonal, 1:1000; R&D Systems, Minneapolis, MN), phospho-eukaryotic elongation factor (eEF) 2 (Thr56), eEF2 (both from Cell signaling, Danvers, MA; 1:1000), actin (rabbit polyclonal 1:5000; Sigma-Aldrich), or tubulin (mouse polyclonal 1:1000; Sigma-Aldrich). Protein detection was with horseradish peroxidase conjugated secondary antibodies (1:2000; Dako) and ECL (Amersham Biosciences Pharmacia). Bands were quantified using Image J 1.32 software (National Institutes of Health) and fold change from mock-infected, calculated and normalized to the fold change in tubulin or actin (18).

Cathepsin D Activity Assay—Cathepsin D activity was measured in cell lysates using a fluorometric cathepsin D activity assay kit (Abcam) in accordance with the manufacturer's instructions. Fluorescence was measured on a Packard Bioscience Fusion™ microplate analyzer. Cathepsin D activity in each lysed sample was expressed as a percentage of a comparative sample that had been treated with an excess (500 μM) of pepstatin A to act as a negative control.

Sample Preparation and iTRAQ labeling—Protein samples were precipitated using ice-cold acetone at −20 °C overnight, harvested by centrifugation at 21,000 × *g* at 4 °C for 20 min (22) and resuspended in 1 M Triethyloammoniumbicarbonate at pH 8.5. Total protein quantification involved the Rc-Dc Quantification Assay (Bio-Rad; UK) according to the manufacturer's instructions. One hundred micrograms of each sample was used for the eight-plex iTRAQ technique (Applied Biosystems, Foster City, CA). These samples were reduced, alkylated, digested, and labeled with iTRAQ reagents according to the manufacturer's protocol (Applied Biosystems), as previously described (22). The labeling of samples was carried out with 15 sets for data analysis. Two independent biological triplicates (D39 labeled with reagents 115, 116, 117, and D39 with pepstatin A labeled with reagents 118, 119, 121) and one biological duplicate (MI, labeled with reagents 113 and 114) were applied (Fig. 1). After incubation at room temperature, labeled samples were combined before being dried in a vacuum concentrator. Fractionation of samples using strong cation exchange on a BioLC HPLC system (Dionex, UK) was used to clean the samples, as well as to reduce their complexity (23). The strong cation exchange fractionation was carried out using a PolySulfoethyl A Column (PolyLC, USA) with a 5 μm particle size, 20 cm length × 2.1 mm diameter, and 200 Å pore size. The system was operated at a flow rate of 0.2 ml·min^{-1} with an injection volume of 120 μl. The mobile phase comprised buffers A and B. Buffer A contained 10 mM KH_2PO_4, 25% acetonitrile at pH 3, and buffer B consisted of 10 mM KH_2PO_4, 25% acetonitrile, and 500 mM KCl, at pH 3. A 60-min gradient was used, which was 5 min at 100% buffer A, followed by ramping from 5% to 30% buffer B over 40 min, then 30% to 100% buffer B over 5 min, and finally holding at 100% buffer A for 5 min. A UV detector

[1] The abbreviations used are: iTRAQ, isobaric tag for relative and absolute quantitation; BMDM, bone marrow-derived macrophage; eEF2, eukaryotic elongation factor 2; FLIP, Fas-associated protein with death domain-like interleukin-1 beta converting enzyme inhibitary protein; Hsp, heat shock protein; MDM, monocyte-derived macrophage; ROS, reactive oxygen species; SOD, superoxide dismutase; $\Delta\psi_m$, mitochondrial inner transmembrane potential.

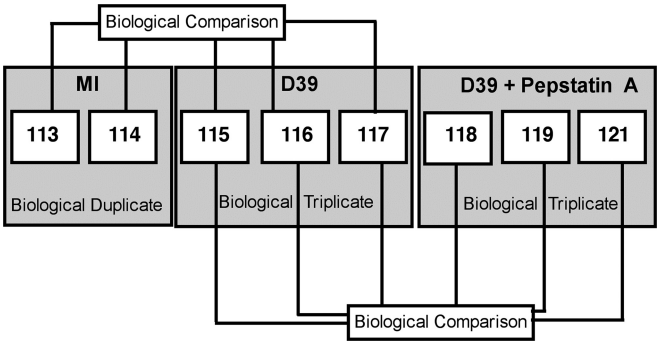

FIG. 1. **Experimental schematic.** A biological duplicate of mock-infected (MI) cells and two biological triplicates of *Streptococcus pneumoniae* exposed cells incubated with vehicle control (D39) or with pepstatin A (D39 + Pepstatin A) were used for analysis.

UVD170U and Chromeleon Software (Dionex, The Netherlands) were used to record the chromatogram. Labeled peptide fractions were collected every minute, and then each fraction was dried in a vacuum concentrator. These dried labeled-peptides were then cleaned up using C_{18} Discovery DSC-18 SPE column (100 μg capacity, Supelco, Sigma) as detailed by Chong and Wright (24) before submission to the mass spectrometry instrument.

LC-MS/MS UHR-TOF Analysis—Tandem mass spectrometry of liquid chromatography (LC)-MS iTRAQ labeled samples was carried out on a maXis hybrid ultra-high resolution quadrupole time-of-flight system (Bruker Daltonics, Coventry UK) coupled to an Ultimate 3000 nano-flow HPLC (Dionex, Surrey, UK) (25). All LC-MS iTRAQ samples were first desalted online using a 5 mm, 300 μm ID LC-Packings C_{18} PepMap trap cartridge under 0.1% trifluoroacetic acid and 3% acetonitrile (ACN) for 15 min, and eluted to a 15 cm, 75 μm ID LC-Packings C_{18} PepMap analytical column in 0.1% formic acid, with an ACN gradient extending from 3% to 95%. Elution was performed on a predefined 70-min gradient program (3–35% ACN) with a 20% wash step (35–95% ACN) as described (26). TOF-MS screening measurements were performed on a predefined 50–2200 *m/z* acquisition window at 2500 TOF summations (approx. 2 Hz) at R (resolution) = 40000 at 622 *m/z*. Collision-induced dissociation MS/MS acquisition were performed over the same 50–2200 *m/z* window at $r = 40{,}000$ at 622 *m/z* with three intensity binned precursors of charge +2 to +4 with at least 2500 counts between 250–1400 *m/z*, deriving from the TOF-MS screening experiment. Accumulation times for tandem MS (MS/MS) were also intensity binned at a maximum of 5000 summations (approximately 1 Hz, if precursor $\leq 2.5 \times 10^3$ ion counts) and a minimum of 2000 summations (approximately 2.5 Hz, if precursor $\geq 2 \times 10^4$ ion counts). An optimized set of isolation windows was used based on the precursor *m/z* to achieve at least 90% precursor recovery; 1.5 *m/z* for $<$ 300 *m/z*, 3 *m/z* for $<$ 500 *m/z*, 4 *m/z* for $<$ 1000 *m/z* and 5.5 *m/z* for $<$ 1400 *m/z*. Selected precursors after fragmentation twice were actively excluded for 90 s from further analysis. To overcome the increased stability because of the iTRAQ labels, collision energies were increased by 10% to optimize for peptide fragmentation.

MS/MS Data Analysis—Data processing of LC-MS/MS samples were first parsed using proprietary vendor analysis software, microTOF Control v 2.3 Service Pack 1, and processing module, Data Analysis v 4.0 Service Pack 2 (all from: Bruker Daltonik GmbH, Bremen Germany). MS/MS data recovery to MGF was processed via an embedded daMGF script. Data were then searched against the International Protein Index (IPI) human database (downloaded from http://www.ebi.ac.uk, on September 2009, with 84,032 protein entries) using a local Phenyx v2.5 (Genebio, Geneva Switzerland) processing cluster at the ChELSI Institute. The search parameters were set as follows: MS tolerance was 0.4 Da and MS/MS tolerances were set at: peptide tolerance 0.2 Da, charge +1, +2, +3, and +4. Minimum peptide length, z-score, maximum *p* value, and AC score were 6, 5.5, 10^{-6}, and 6, respectively. The enzyme mode for searching was trypsin, permitting up to two missed cleavages. Modifications were performed as follows: eight-plex iTRAQ mass shifts (+304 Da, K and N-term) as fixed modification, cys CAM (+57 Da) as fixed modification on the C residue, and oxidation of methionine (+16 Da) as variable modification on the M residue. These data were then searched for within the reversed IPI human database to estimate the false positive peptide discovery rate using the formula, false positive peptide discovery rate = 2 decoy_hits/(decoy_hits + true_hits), as detailed elsewhere (27). Processed data were exported to Excel (Microsoft 2008, USA) for further analyses *via* Phenyx local export to retrieve peptide identification data and reporter intensity values for each separately identified peptide. Peptide data and intensity values were parsed locally to Mathematica v7.0 (Wolfram Research, Oxfordshire UK) with more details found in Pham *et al.* (28). From this, only peptides with $\geq$2 peptide identifications were used for both identification and quantitation. Functional classification of the identified proteins was generated through use of Ingenuity Pathway Analysis (Ingenuity ® Systems, www.ingenuity.com).

Measurement of Reactive Oxygen Species (ROS)—Production of intracellular ROS was measured using the cell permeable molecule 2′, 7′-dichloro-dihydrofluorescein diacetate (DCF; Sigma-Aldrich) (29). Macrophages were pre-incubated with 10 μM DCF for 30 min before infection for the indicated time periods. Cells were washed in phosphate-buffered saline (PBS) then analyzed by flow cytometry.

Measurement of Mitochondrial Inner Transmembrane Potential ($\Delta\psi_m$)—To detect loss of $\Delta\psi_m$ at the required time-points, cells were incubated with 10 μM 5,5′, 6,6′-tetrachloro-1, 1′, 3,3′ tetraethylbenzimidazolocarbocyanine iodide (JC-1; Sigma-Aldrich) for 15 min and analyzed by flow cytometry. Loss of $\Delta\psi_m$ was demonstrated by a loss of fluorescence on the FL-2 channel as previously described (18).

Mouse Infection Model—eEF2 kinase knockout or littermate control, female C57Bl6 mice at 8–14 weeks of age, received 5×10^5 colony forming units of type 1 *S. pneumoniae* via intratracheal instillation and 24 h lungs were harvested, homogenized and bacterial colony counts obtained by the surface viable count method (17). All experiments were performed in accordance with the UK Animals Act, authorized under a UK Home Office License, and approved by the animal project review committee of the University of Sheffield.

Statistical Analysis—Macrophage data was recorded as means ± S.E. of the mean (se) unless otherwise stated. Statistical testing was performed using Prism® 5.02 software (GraphPad Software Inc.) with relevant statistical tests described in the figure legends. Significance was defined as $p < 0.05$.

Proteomic values were recorded as median values. For the proteomic analysis we used two biological triplicates (for D39 and D39+PepstatinA). To identify differentially expressed proteins we performed *t* test comparisons between the iTRAQ reporter ions' intensities (considering all MS/MS spectrum for a given protein). Therefore significance increased with the number of MS/MS spectra obtained for a protein. To be significant all t-tests of each pairwise comparison were less than $\alpha = 0.05$, with a false discovery rate of $\leq$1% (data not shown).

RESULTS

Macrophage Ingestion of S. pneumoniae is Associated with Cathepsin D Activation—Following phagocytosis of *Streptococcus pneumoniae*, the fusion of lysosomes with the phagosome, generates a phagolysosome where bacteria are killed (30). Of the proteolytic enzymes present, cathepsin D is the

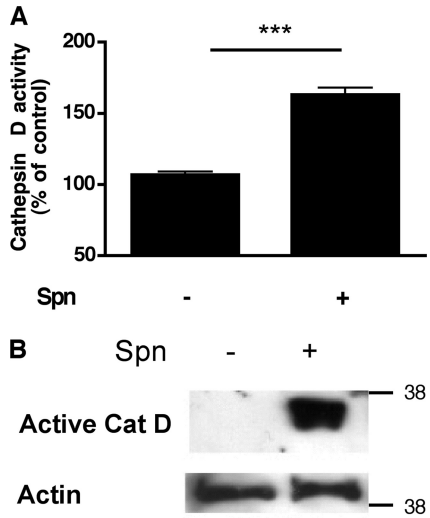

FIG. 2. **Infection with *Streptococcus pneumoniae* is associated with activation of cathepsin D in macrophages.** *A*, Cathepsin D activity was measured in whole-cell lysates at 16 h in mock-infected (Spn-), or *Streptococcus pneumoniae* exposed (Spn+) monocyte-derived macrophages, $n = 4$, *** = $p < 0.001$, Student's t test. *B*, Western blot of differentiated THP-1 cells 16 h after mock-infection (Spn-) or exposure to *Streptococcus pneumoniae* (Spn+). The blot is representative of three independent infections.

most abundant of the cathepsin proteases (9). To confirm that *S. pneumoniae* infection activated cathepsin D in MDM, a fluorogenic substrate of cathepsin D was used as a marker of activation. D39 infected cells showed significant activation of cathepsin D at 16 h postinfection, compared with mock-infected cells (Fig. 2*A*). This result was corroborated by Western blot on differentiated THP-1 cells 16 h postinfection (Fig. 2*B*). Infection caused an increase in the active 35 kDa form of cathepsin D (31, 32).

A Quantitative Proteomic Approach Demonstrates a Wide Range of Proteins are Regulated by Cathepsin D Following Exposure to S. pneumoniae—Cathepsin D activates multiple cellular pathways (33–35). In view of the broad substrate range of cathepsin D (36), we opted to perform analysis using iTRAQ to allow an unbiased quantitative proteomic approach to examine how cathepsin D activation regulated the macrophage proteome during *S. pneumoniae* infection. Macrophages were exposed to *S. pneumoniae* (D39) in the presence or absence of the cathepsin D inhibitor pepstatin A (PepA). Cells were analyzed 16 h postinfection, in the late stages of the antimicrobial response, a time at which a program of apoptosis is initiated and provides a late increment to bacterial killing in this model (18). All MS/MS data were submitted to our Phenyx server and as a result, 15,734 peptides corresponding to 679 proteins were identified (supplemental Tables S1 and S2). A false positive peptide discovery rate of 1.1% was detected. The numbers of peptides contributing to each detected protein are also presented (supplemental Table S1). Example spectra for iTRAQ labeled peptide fragmentation of high and low intensities are also shown (supplemental Fig. 1).

To better assess cathepsin D regulated proteins involved in apoptosis, we used a statistical method based on peptide-level intensities of iTRAQ reporters to determine which proteins show differential regulation to statistically significant levels during infection in the presence or absence of cathepsins D activation. The application of median-corrected intensities at the peptide level, rather than protein level, provides more accuracy for distinguishing smaller changes in protein expression (28). All proteins quantified here are presented showing the relationship between relative abundance ratios and p values (from t test) to give an indication of statistical significance.

We focused our attention on the comparison of biological triplicates of *S. pneumoniae* infection in the presence or absence of pepstatin A (D39+pepstatin A *versus* D39) to identify cathepsin D regulated proteins. We assumed that most cathepsin D regulated proteins would in fact also be differentially regulated by infection, because our previous data showed there was little cathepsin D activation in unstimulated macrophages in the absence of exposure to *S. pneumoniae* (15). Although we planned to use subsequent Western blotting to validate this our experimental protocol using an 8-plex iTRAQ technique allowed us to include a biological duplicate of mock-infected cells for comparison with the biological triplicate of *S. pneumoniae* challenged cells incubated without pepstatin A (MI *versus* D39) (see Fig. 1). If we considered proteins identified by at least two distinct peptides and ratios with p values ≤ 0.05, 18 proteins with differential expression regulated by cathepsin D were identified (Table I and supplementary Table S3). Using these criteria, we identified 26 proteins that were differentially expressed following exposure to *S. pneumoniae* (supplemental Table S4).

Of the 18 proteins (2.7% of the 679) that showed cathepsin D mediated regulation (Table I), ten proteins were elevated and eight proteins reduced in D39 + pepstatin A samples *versus* D39. Functional classification of these 18 proteins using Ingenuity Pathway Analysis showed that they could be grouped into a number of different functional categories, including cellular assembly and organization, and cell morphology (Table II). However, the most significant classification grouping was that of cell death. Indeed, 12 (66.7%) of the 18 differentially expressed proteins were identified as being directly or indirectly involved in cell death processes (Table II).

Given that cathepsin D has previously been implicated in the regulation of apoptosis pathways in myeloid cells (13), and we have shown macrophage apoptosis in response to *S. pneumoniae* is necessary for bactericidal clearance in this model (17, 18), several of these proteins were investigated further to determine how cathepsin D activation might influence pathways involved in the regulation of macrophage apoptosis during *S. pneumoniae* exposure.

Validation of Proteomic Data—Differentiated THP-1 cells, under the same conditions as used for the iTRAQ analysis, were lysed and Western blots performed to verify the pro-

TABLE I

Proteins showing significant differential expression in D39 + pepstatin A samples versus D39. A list of identifying peptide sequences can be found in supplemental Table S1

AC	Name	Gene	# MS/MS spectra	# distinct peptides	D39+Pepstatin A vs D39 (log)	D39+Pepstatin A vs D39 (fold change)	*p* value
IPI00003362	HSPA5 PROTEIN	HSPA5	265	27	−0.135813434	−1.145468168	0.005871795
IPI00010796	PROTEIN DISULFIDE-ISOMERASE	P4HB	168	29	−0.182633409	−1.200374281	9.08145E-05
IPI00027463	PROTEIN S100-A6	S100A6	34	2	0.621278866	1.861306883	3.12998E-07
IPI00032313	PROTEIN S100-A4	S100A4	35	5	0.542251927	1.719875539	1.98609E-06
IPI00186290	EEF2 ELONGATION FACTOR 2	EEF2	5	2	0.83084303	2.295252891	5.45704E-05
IPI00217467	HISTONE H1.4	HIST1H1E	28	10	0.251455004	1.285895038	0.001929287
IPI00414676	HEAT SHOCK PROTEIN HSP 90-BETA	HSP90AB1	162	16	−0.183289861	−1.201162528	0.001015541
IPI00418471	VIMENTIN	VIM	786	40	−0.194527203	−1.214736527	7.26613E-10
IPI00453473	HISTONE H4	HIST1H4L	232	8	−0.117458357	−1.124634796	0.010240815
IPI00639931	ISOFORM 2 OF ADENYLYL CYCLASE-ASSOCIATED PROTEIN 1	CAP1	317	5	0.222439155	1.249119814	5.35533E-07
IPI00646773	ISOFORM 2 OF GELSOLIN	GSN	130	20	0.202269345	1.22417769	0.000514948
IPI00784295	ISOFORM 1 OF HEAT SHOCK PROTEIN HSP 90-ALPHA	HSP90AA1	88	8	−0.196686965	−1.217362904	0.006951707
IPI00894365	CDNA FLJ52842, HIGHLY SIMILAR TO ACTIN, CYTOPLASMIC 1	ACTB	205	13	0.272662307	1.313456624	5.37642E-07
IPI00896370	SUPEROXIDE DISMUTASE [MN], MITOCHONDRIAL	SOD2	18	4	−0.517671504	−1.678115611	0.004875778
IPI00908876	CDNA FLJ50830, HIGHLY SIMILAR TO SERUM ALBUMIN	ALB	8	3	−0.610283479	−1.840953196	0.001745351
IPI00922693	CDNA FLJ53662, HIGHLY SIMILAR TO ACTIN, ALPHA SKELETAL MUSCLE	ACTB	139	2	0.229450796	1.257908972	5.01643E-06
IPI00930226	CDNA FLJ57283, HIGHLY SIMILAR TO ACTIN, CYTOPLASMIC 2	ACTG1	374	24	0.211742014	1.235829017	1.46192E-12
IPI00939159	ADENYLYL CYCLASE-ASSOCIATED PROTEIN	CAP1	268	4	0.193093886	1.212996672	1.47374E-05

TABLE II

Top five functional classifications (by p value) of the 18 proteins regulated by cathepsin D in infection (D39 + pepstatin A vs. D39), as analysed by Ingenuity Pathway Analysis

Category	No. of proteins	*p* value	Molecules
Cell Death	12	4.34E-09-3.09E-02	P4HB, SOD2, S100A6, S100A4, HSP90AA1, ACTB, HSP90AB1, VIM, ALB, GSN, HSPA5, EEF2
Cell Morphology	8	5.85E-07-4.52E-02	CAP1, SOD2, S100A4, HSP90AA1, ACTB, VIM, ALB, GSN
Cellular Development	9	4.01E-06-4.43E-02	CAP1, SOD2, S100A4, HSP90AA1, VIM, ALB, GSN, HSPA5, HIST4H4
Cellular Assembly and Organization	11	1.2E-05-4.52E-02	ACTG1, CAP1, SOD2, S100A4, HSP90AA1, ACTB, ALB, HIST1H1E, VIM, GSN, HSPA5
Post-Translational Modification	7	3.4E-05-3.63E-02	P4HB, SOD2, HSP90AA1, HSP90AB1, ALB, GSN, HSPA5

teomics findings. In total, five proteins were examined further, all known to have links to cell death processes. In every case, Western blot analysis with densitometry performed on four biological replicates confirmed the findings of the iTRAQ analysis, providing evidence, not only that each protein was differentially expressed in the presence of pepstatin A, but also that each protein was differentially regulated by infection. Superoxide dismutase (SOD)-2 (decreased 1.68-fold, $p = 0.005$ in D39+pepstatin A *versus* D39 by iTRAQ analysis) and glucose sensitive heat shock protein (Hsp) A5, also termed glucose-regulated protein of 78 kDa (Grp78) or BiP, (decreased 1.15-fold, $p = 0.006$ in D39+pepstatin A *versus* D39 by iTRAQ analysis), were both elevated in infection, but up-regulation was reversed by pepstatin A indicating a role for cathepsin D in protein up-regulation (Figs. 3*A* and 3*B*). In contrast, the actin regulatory protein gelsolin (up-regulated 1.22-fold, $p = 0.0005$ in D39+pepstatin A *versus* D39 by iTRAQ analysis) and the translation factor eukaryotic elongation factor (eEF)2 (up-regulated 2.30-fold, $p = 0.00005$ in D39+pepstatin A *versus* D39 by iTRAQ analysis) were down-regulated by Western blot following *S. pneumoniae* exposure, a reduction that was blocked by pepstatin, implicating cathepsin D in the down-regulation observed (Figs. 4*A* and 4*B*). A fifth protein, the calcium binding protein, which enhances the transcriptional activity of the tumor suppressor p53 (37) and can increase transcription of caspase 3 (38), S100A6

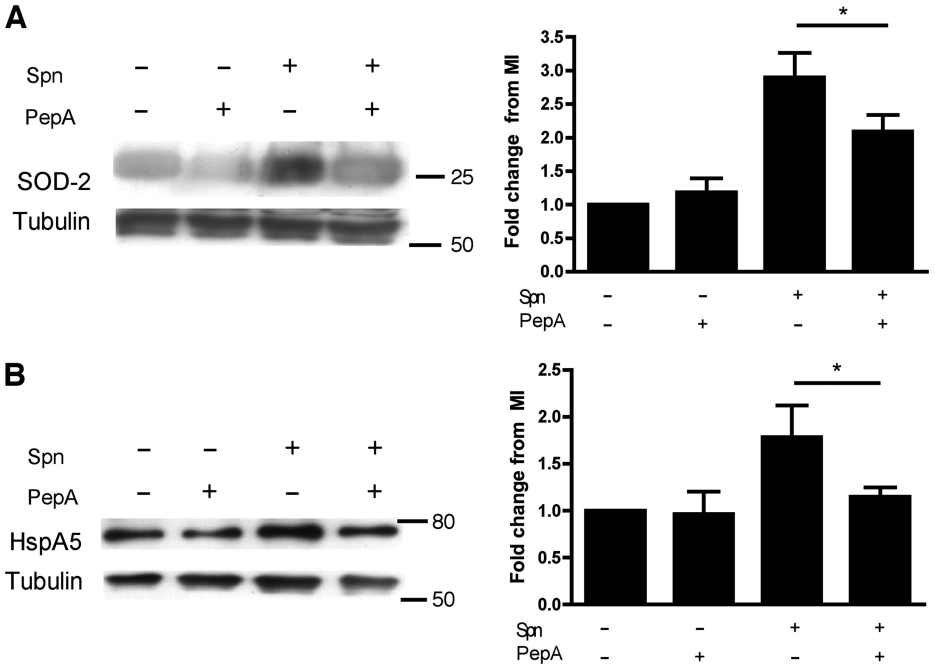

FIG. 3. **Validation of iTRAQ analysis for SOD-2 and HspA5 in differentiated THP-1 macrophages.** Representative Western blots of total protein from mock-infected (Spn-) or *Streptococcus pneumoniae* exposed (Spn+) differentiated THP-1 macrophages, 16 h after infection, cultured in the presence (+) or absence (-) of pepstatin A (PepA), probed for (*A*) superoxide dismutase-2 (SOD-2) or (*B*) heat shock protein A5 (HspA5). Densitometry was carried out on each Western blot and each protein's fold change was compared relative to the mock-infected (MI) level after adjustment for any fold change in tubulin, $n = 4$ * = $p < 0.05$, 1-way ANOVA with Bonferroni post-test.

or calcyclin (up-regulated 1.86-fold, $p = 0.0000003$ in D39+pepstatin A *versus* D39 by iTRAQ analysis), was up-regulated during infection, but in this case pepstatin A treatment resulted in further up-regulation (Fig. 4*C*). These results indicate that the iTRAQ analysis appeared to have identified potential cathepsin D targets with known roles in the regulation of cell survival.

Pharmacological inhibition of cathepsin D could however in theory have off-target effects. To confirm our findings further we also repeated Western blots and densitometry on BMDM derived from cathepsin D deficient infant mice or their wild-type littermates. This confirmed cathepsin D dependent up-regulation of SOD-2 and HspA5 (Figs. 5*A* and 5*B*) and down-regulation of gelsolin and eEF2 (Figs. 6*A* and 5*B*) following infection, with an increase in S100A6 following infection that was further increased in the absence of cathepsin D (Fig. 6*C*).

Superoxide Dismutase (SOD)-2 is Up-regulated in Macrophages During S. pneumoniae Infection in a Cathepsin D Dependent Manner—The first protein of interest to be investigated further was SOD-2. SOD-2 is a protein which protects mitochondria against oxidative stress (39). The iTRAQ analysis, verified by Western blots, documented cathepsin D-dependent SOD-2 up-regulation. To validate these results in primary cells, and to elucidate the potential kinetics of this up-regulation, a timecourse was performed using MDM. Western blot analysis demonstrated that *S. pneumoniae* infection dramatically increased SOD-2 levels from 8 h postinfection (Fig. 7*A*). *S. pneumoniae* exposed cells treated with pepstatin A showed reduced SOD-2 expression compared with nontreated cells. Enhanced expression of SOD-2 is considered one of the first lines of defense against excess levels of ROS, which are produced by activated macrophages (40, 41), and SOD-2 is known to be differentially expressed following bacterial infection (42, 43). To confirm enhanced ROS production in our model and relate its kinetics to SOD-2 up-regulation, MDM production of ROS was measured using a fluorescent reporter for ROS, DCF. ROS production increased from 8 h after exposure to *S. pneumoniae*. (Fig. 7*B*). The kinetics of ROS production mirrored the up-regulation of mitochondrial SOD-2.

Gelsolin is Down-regulated by Cathepsin D in Macrophages After S. pneumoniae Infection—The next protein of interest to be studied further was the actin regulatory protein gelsolin (44). Gelsolin reduces apoptosis both at the level of mitochondrial outer membrane permeabilization (45) and caspase activation (46, 47). A time course of gelsolin expression in MDM revealed down-regulation in a cathepsin D-dependent fashion from 12 h post-infection, with maximal down-regulation observed at 16 h (Fig. 8*A*). The maximal down-regulation coincided with cytochrome *c* translocation to the cytosol (Fig. 8*B*), a hallmark of mitochondrial outer membrane permeabilization, which is widely recognized as being the point of no return in an apoptotic program of death (48). These data suggest a model in which cathepsin D acts to down-regulate gelsolin, thus contributing to the destabilization of the mitochondria, leading to apoptosis.

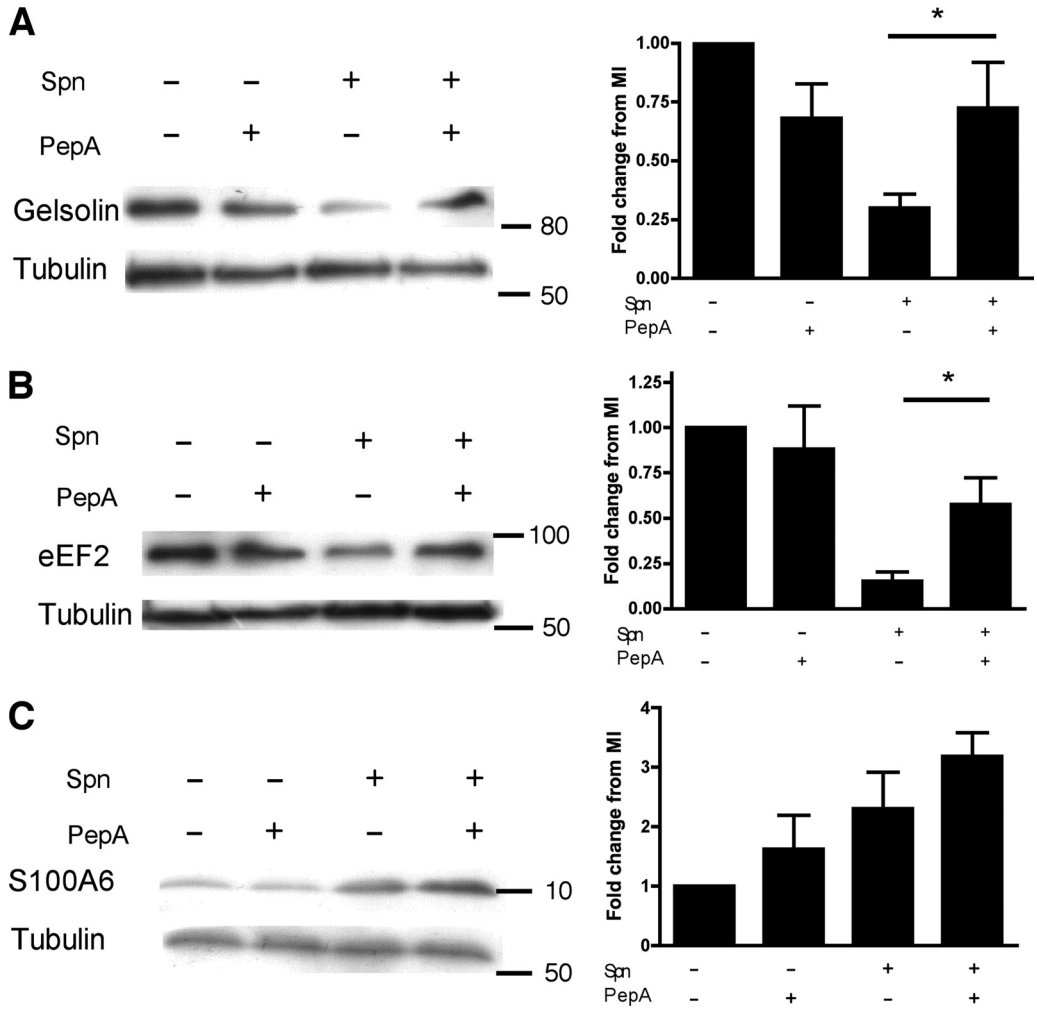

FIG. 4. **Validation of iTRAQ analysis for gelsolin, eukaryotic elongation factor 2 (eEF2) and calcyclin (S100A6) in differentiated THP-1 macrophages.** Representative Western blots of total protein from mock-infected (Spn-) or *Streptococcus pneumoniae* exposed (Spn+) differentiated THP-1 macrophages in the presence (+) or absence (-) of pepstatin A (PepA) probed for (*A*) gelsolin, (*B*) eukaryotic elongation factor 2 (eEF2) or (*C*) calcyclin (S100A6) 16 h postinfection. Densitometry was carried out and each protein's fold change was compared relative to the mock-infected (MI) level after adjustment for any fold change in tubulin, $n = 4$ * = $p < 0.05$, 1-way ANOVA with Bonferroni's post-test.

Cathepsin D Induces Eukaryotic Elongation Factor 2 (eEF2) Down-regulation Enhancing Apoptosis and Bacterial Killing—eEF2 was also identified as a factor down-regulated by cathepsin D. eEF2 was reduced 16–20 h post-infection in a cathepsin D-dependent fashion (Fig. 9*A*). Proteins with short half-lives, such as Mcl-1, a key regulator of macrophage susceptibility to apoptosis, including during *S. pneumoniae* infection, are exquisitely sensitive to alterations in protein translation (18, 49, 50). eEF2 activity is negatively regulated by eEF2 kinase, which prevents protein translation via the phosphorylation of eEF2 (51). During cellular stress, eEF2 kinase is activated with the purpose of reducing protein synthesis and conserving cellular energy sources (21, 52). We found an increase in eEF2 kinase activity 12–16 h post-infection (Fig. 9*B*), but there was no evidence that this was regulated by cathepsin D activation (data not shown). By studying macrophages deficient in eEF2 kinase we could examine the role of eEF2 using a system where eEF2 activity is inappropriately prolonged in the absence of the normal inhibitory effect of phosphorylation. As compared with wild-type BMDM, BMDM from eEF2 kinase$^{-/-}$ mice (53), maintained Mcl-1 levels (Fig. 9*C*) and had delayed dissipation of $\Delta\psi_m$ after *S. pneumoniae* infection (Figs. 9*D* and 9*E*). We conclude from these results that inactivation of eEF2-dependent protein translation is required for Mcl-1 down-regulation after *S. pneumoniae* infection and that cathepsin D induced down-regulation of eEF2 can drive apoptosis by reducing the translation of Mcl-1.

One of the consequences of macrophage apoptosis during *S. pneumoniae* infection is to increase bacterial killing (18). To test whether our proteomic screen was identifying targets that could link macrophage apoptosis with bacterial killing, we measured bacterial clearance in the eEF2 kinase$^{-/-}$ mice that had preservation of Mcl-1 and delayed macrophage apoptosis. Pneumococcal clearance was reduced by ~0.5 log in

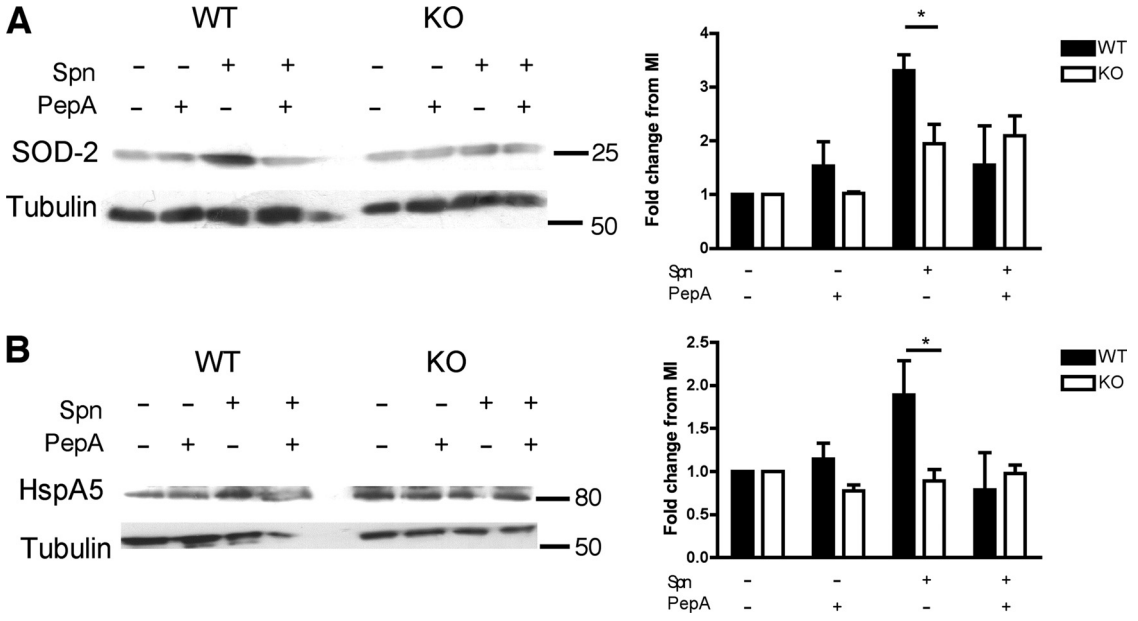

FIG. 5. **Cathepsin D deficient macrophages validate iTRAQ findings for SOD-2 and HspA5.** Representative Western blots for (*A*) SOD-2 and (*B*) HspA5 from wild-type (WT) and Cathepsin D knockout (KO) BMDMs 16 h after mock- infection (Spn-) or exposure to *Streptococcus pneumoniae* (Spn+), in the presence (+) or absence (-) of pepstatin A (PepA). Blots are representative of three independent experiments. Densitometry was carried out and each protein's fold change was calculated relative to the mock-infected (MI) level after adjustment for any fold change in tubulin, $n = 3$ * = $p < 0.05$, 2-way ANOVA with Bonferroni post-test.

eEF2 kinase$^{-/-}$ mouse lungs (Fig. 10). This difference reflects the relatively modest effect on apoptosis of maintaining active eEF2 by inhibition of eEF2 phosphorylation, because cathepsin D activation still induced eEF2 down-regulation and also the fact that cathepsin D can exert its effects on macrophage survival at several points, as this screen has shown. However the reduction in bacterial killing did establish that our screen identified proteins that not only influenced macrophage apoptosis but also bacterial clearance *in vivo*.

DISCUSSION

To better understand how the co-ordination of antimicrobial host defense in the phagolysosome regulates macrophage survival we have examined how activation of one of the most abundant lysosomal proteases, cathepsin D, influences the macrophage proteome (9). We show that a range of proteins are differentially expressed in the presence of cathepsin D, with a high proportion predicted to impact the regulation of the mitochondrial pathway of apoptosis. Western blotting validated a number of the proteins identified by proteomic analysis and we found evidence that these changes fit well with the temporal sequence of molecular events that are associated with macrophage apoptosis during *Streptococcus pneumoniae* infection, a process we have recently demonstrated involves cathepsin D activation (15).

To identify cathepsin D regulated proteins after the internalization of *S. pneumoniae* into macrophage phagolysosomes we have focused on comparison of biological triplicates of macrophages exposed to *S. pneumoniae* in the presence or absence of the cathepsin D inhibitor pepstatin A. We focused on this comparison because our previous data showed that there was limited activation of cathepsin D in unstimulated macrophages in the absence of exposure to *S. pneumoniae* (15). Our approach was not based on a fold cut-off because our previous results suggest this approach can have limitations (28). Instead our statistical approach involved recently described methodology for quantitative proteomic analysis (25, 54, 55). The use of median-corrected intensities and *t*-tests at the peptide level rather than at the protein level offer higher significance levels and allow the detection of smaller fold changes (28). We believe this was an appropriate approach in the current study. Small fold changes in regulators of apoptosis can have significant effects on phenotype. For example we previously found that a 1.3-fold change in the anti-apoptotic protein Mcl-1 was associated with a prosurvival effect for the early stages of microbial killing by macrophages and helped the cell withstand the proapoptotic effects of increased cellular stress (18). We were therefore keen not to exclude proteins with low levels of differential fold regulation in our model. In addition we have shown iTRAQ can suppress fold change (25, 56) so we elected to identify targets with the iTRAQ approach, without excluding those with lower fold changes, but to validate these vigorously by Western blotting.

The validation approach was also critical to prove that the differentially regulated proteins we identified in cells exposed to *S. pneumoniae*, in the presence or absence of pepstatin A, were also differentially regulated by infection itself. Although

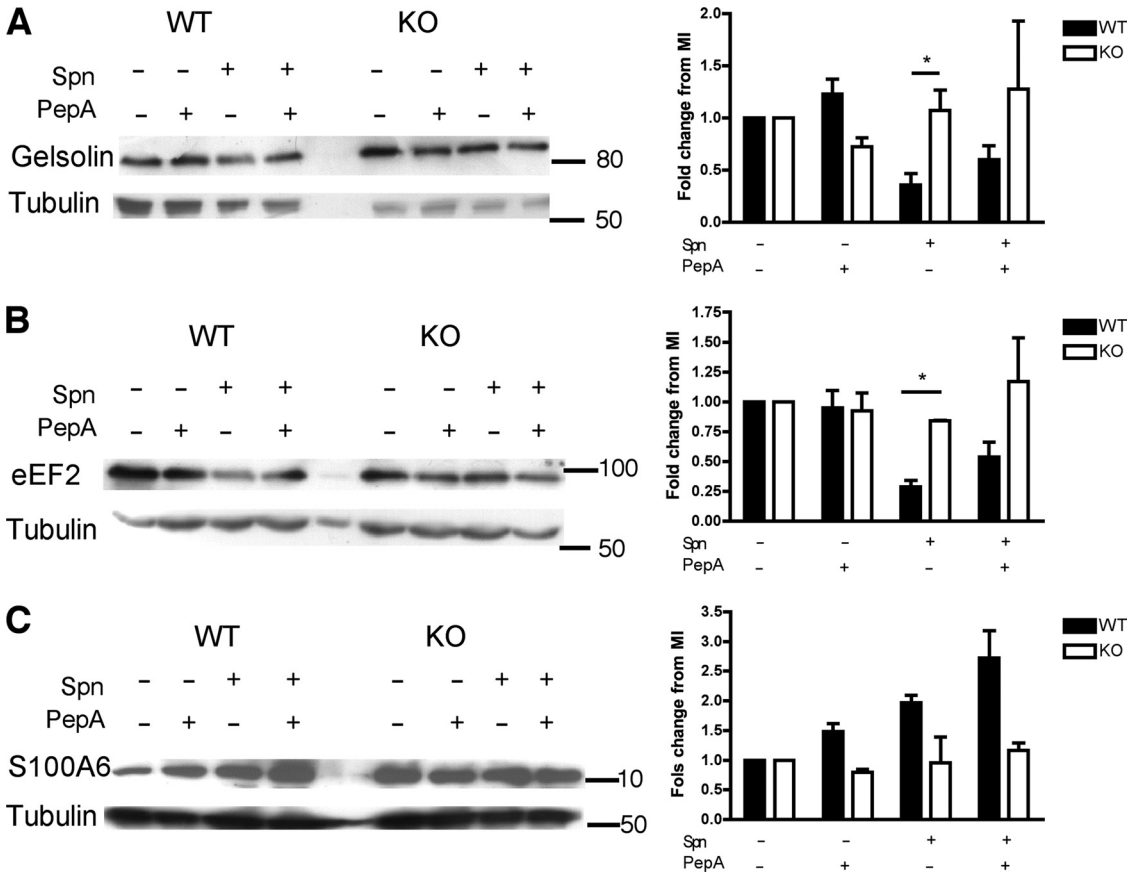

FIG. 6. **Cathepsin D deficient macrophages validate iTRAQ findings for gelsolin, eEF2 and S100A6.** Representative Western blots for (*A*) gelsolin (*B*) eukaryotic elongation factor 2 (eEF2), and (*C*) S100A6 from wild-type (WT) and Cathepsin D knockout (KO) BMDMs 16 h after mock-infection (Spn-) or *Streptococcus pneumoniae* exposure (Spn+), in the presence (+) or absence (-) of pepstatin A. Blots are representative of three independent experiments. Densitometry was carried out and each protein's fold change was calculated relative to the mock-infected (MI) levels after adjustment for any fold change in tubulin, $n = 3$ * = $p < 0.05$, 2-way ANOVA with Bonferroni post-test.

we believed there was not significant cathepsin D activity in unstimulated mock-infected cells our comparison of the mock-infected biological replicate *versus* the *S. pneumoniae* exposed triplicate only identified two of our five targets (with a third having a *p* value that almost reached statistical significance $p = 0.058$, data not shown) but this appeared to reflect the stringency of our statistical approach because all five proteins were differentially regulated by Western blotting. Thus our approach showed it could identify relevant targets when biological triplicates were compared but its sensitivity was reduced when a biological duplicate was used. On the other hand the variation between the biological duplicates or triplicates was much less than the variation between experimental conditions suggesting that those differentially regulated proteins represented were unlikely to be false positives (supplemental Fig. S2).

Studies of the macrophage transcriptome in response to *Streptococcus* spp. reveal early up-regulation of multiple genes involved in immune responses, including those involved in the regulation of apoptosis (57, 58). At our late time point after bacterial challenge our analysis did not identify many proteins with primary host defense functions, but confirmed that many proteins regulating cell death pathways were prominently regulated. Similar findings have been found following challenge of macrophages with viruses such as Influenza A virus and epithelial cells with respiratory viruses, with several regulators of apoptosis, that we identified, also showing differential regulation in these studies (59, 60).

Cathepsin D activity is maximal at low pH with a broad substrate range but the majority of the proteins we identified as being regulated by cathepsin D are not localized to the phagolysosmal compartment (36, 61). The proteomic approach we employed does not identify cleavage events and therefore does not characterize the cell degradome, unlike some recently described approaches (62). The changes to the cell proteome are therefore likely to reflect a broad range of indirect effects. Many of the proteins were up-regulated, emphasizing that direct enzymatic degradation of targets was not the sole mechanism. The findings are in line with recent data which emphasize that key cell proteases active during apoptosis, such as caspases, can induce extensive changes

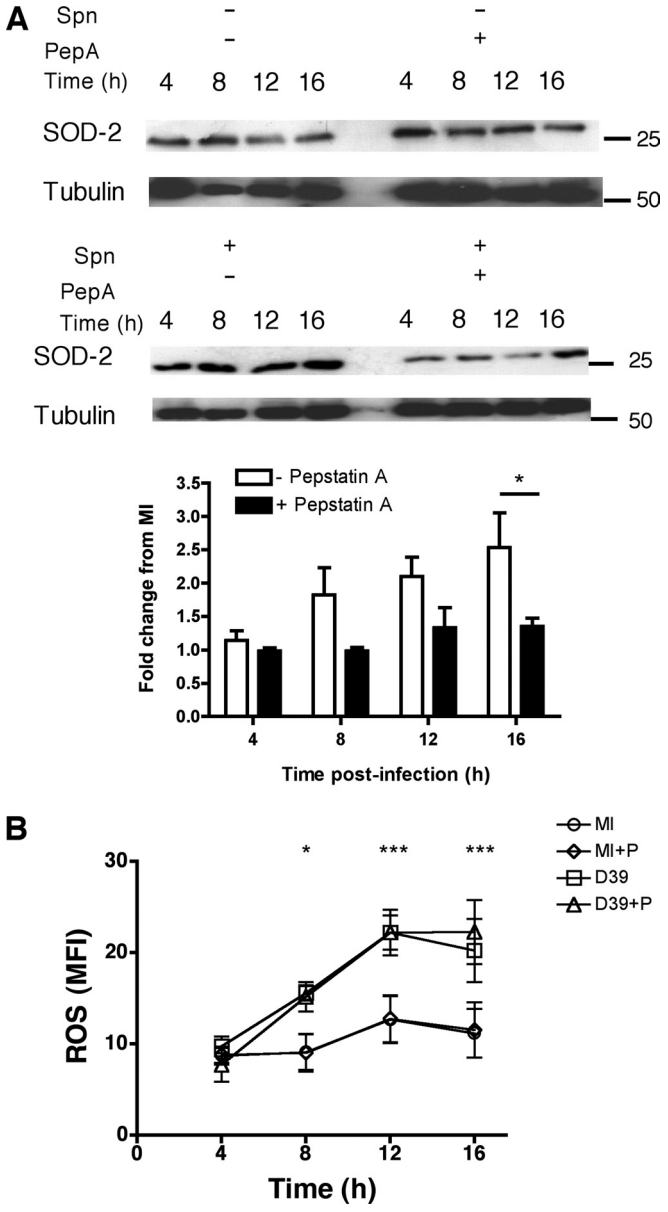

FIG. 7. **Streptococcus pneumoniae infection induces cathepsin D dependent up-regulation of superoxide dismutase-2 (SOD-2).** *A*, Representative Western blots probed for superoxide dismutase-2 (SOD-2) from mock-infected (Spn-) or *Streptococcus pneumoniae* exposed (Spn+) monocyte-derived macrophages (MDM) cultured in the presence (+) or absence (-) of pepstatin A (PepA) at the designated time points after challenge. Densitometry was carried out and fold change was calculated relative to the mock-infected (MI) level after adjustment for any fold change in tubulin, $n = 3$. *B*, Intracellular ROS was measured at the indicated timepoints in MDM, mock-infected (MI) or *Streptococcus pneumoniae* exposed (D39), in the presence of vehicle control or pepstatin A (+P). Data are from six separate donors. * $p < 0.05$, *** $p < 0.001$, 2-way ANOVA with Bonferroni post-test, comparing MI *versus* D39.

to the cell proteome not just through the degradation of protein targets but also indirectly by altering gene transcription and protein-protein interactions (62).

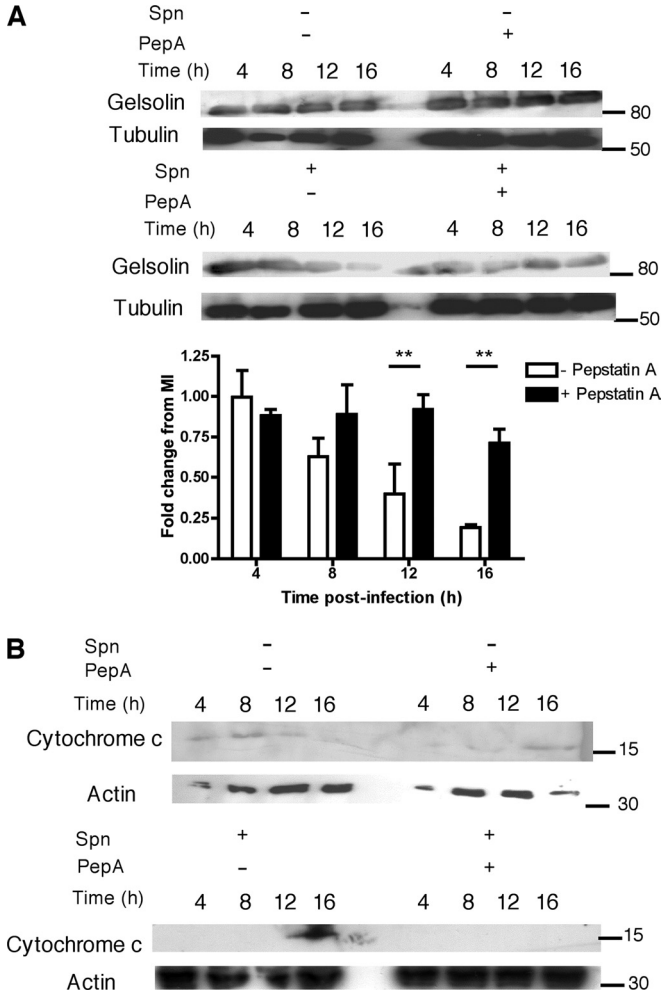

FIG. 8. **Streptococcus pneumoniae infection induces cathepsin D dependent down-regulation of gelsolin.** *A*, Representative Western blots probed for gelsolin from mock-infected (Spn-) or *Streptococcus pneumoniae* exposed (Spn+) monocyte-derived macrophages (MDM) cultured in the presence (+) or absence (-) of pepstatin A (PepA) for the indicated time periods. Densitometry was carried out and fold change was calculated using mock-infected (MI) levels after adjustment for any fold change in tubulin, $n = 3$, ** $p < 0.01$, 2-way ANOVA with Bonferroni post-test. *B*, Cytosolic fractions were obtained from mock-infected (Spn-) or *Streptococcus pneumoniae* exposed (Spn+) monocyte-derived macrophages (MDM) at the designated time points. Western blots were probed for cytochrome *c*, and actin was used as a cytosolic loading control. The blots are representative of three independent experiments.

The data set of proteins regulated by cathepsin D is enriched for proteins predicted to influence a variety of cell death pathways. We have previously shown ROS are not required for effective killing of *S. pneumoniae* (63). SOD-2 converts superoxide anions into hydrogen peroxide (41), but will not influence bacterial killing. Converting superoxide to hydrogen peroxide does not prevent apoptosis since both species can induce apoptosis (64, 65). However by limiting the concentration of superoxide SOD-2 may enable preferential permeabilization of the outer mitochondrial membrane

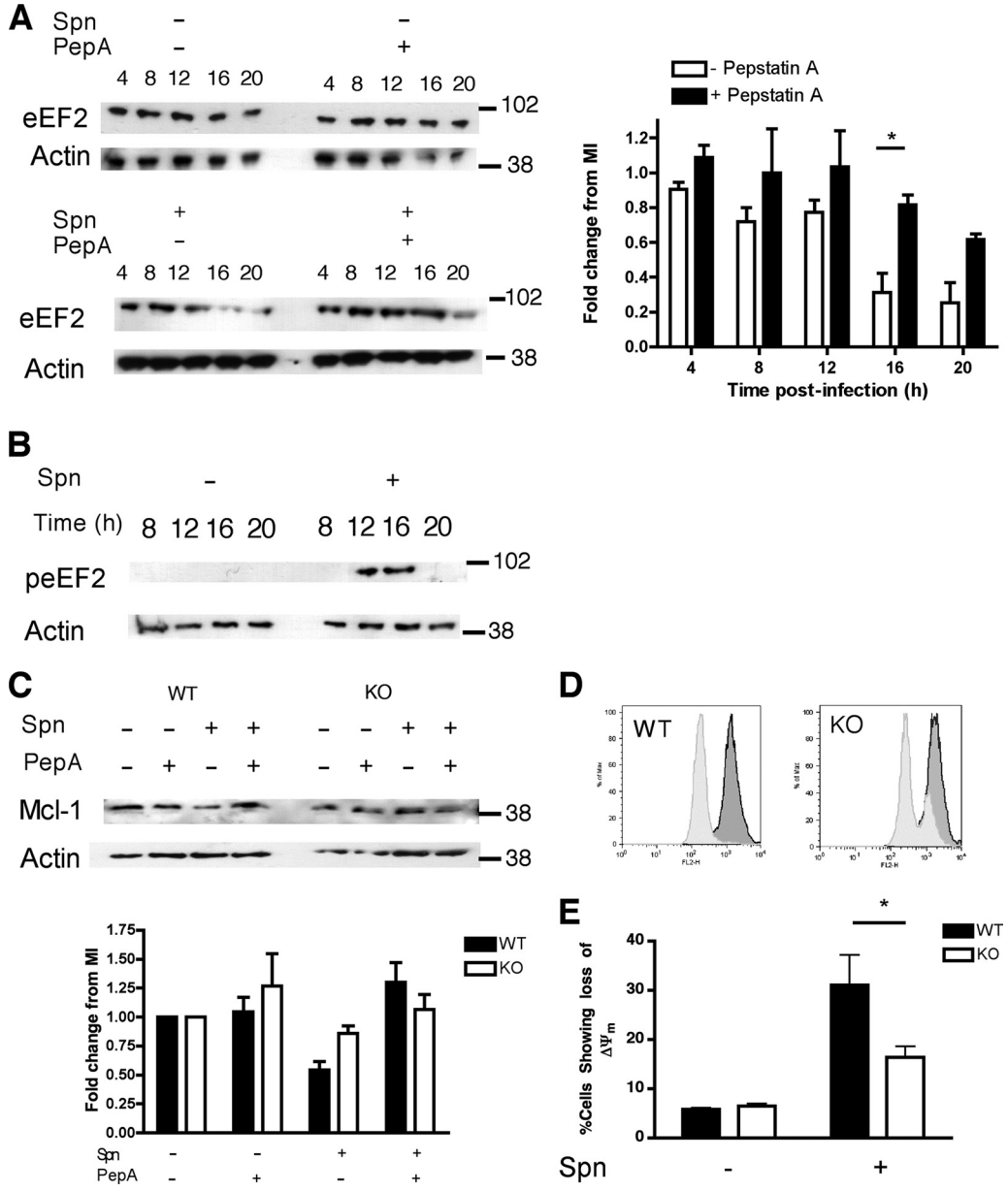

FIG. 9. **Cathepsin D-mediated down-regulation of eukaryotic elongation factor 2 (eEF2) has functional consequences for the regulation of the mitochondrial pathway of apoptosis.** *A*, Western blots of total protein from mock-infected (Spn-) or *Streptococcus pneumoniae* exposed (Spn+) differentiated THP-1 cells at the designated time points in the presence (+) or absence (-) of pepstatin A (PepA) were probed for eukaryotic elongation factor 2 (eEF2). The blots depicted are representative of three independent experiments. Densitometry was carried out and fold change was calculated using the mock-infected (MI) level after adjustment for any fold change in actin, $n = 3$, * $p <$ 0.05, 2-way ANOVA with Bonferroni post-test. *B*, Western blots probed for phospho-eEF2 (peEF2) from Spn- or Spn+ differentiated THP-1 cells at the indicated time points after bacterial challenge. The blots are representative of three independent experiments. *C*, Western blot of protein probed for myeloid cell leukemia sequence (Mcl)-1 from wild-type (WT) or eEF2 kinase knock-out (KO) bone marrow-derived macrophages (BMDM), mock-infected (Spn-) or challenged with *Streptococcus pneumoniae* (Spn+), in the presence (+) or absence (-) of pepstatin A (PepA) and cultured for 16 h. The blots are representative of three independent experiments. Densitometry was carried out and fold change was calculated using mock-infected (MI) levels after adjustment for any fold change in actin, $n = 3$, * $p < 0.05$, 1-way ANOVA with Dunnett's post-test *versus* MI. *D*, Representative histograms and (*E*) pooled data from JC-1 staining of BMDMs expressing (WT) or deficient (KO) in eEF2 kinase. In the histograms dark gray fill represents Spn-, light gray fills Spn+. The pooled data shows the percentage of cells showing loss of inner mitochondrial transmembrane potential ($\Delta\psi_m$), $n = 3$, * $= p < 0.05$, 2-way ANOVA with Bonferroni post-test.

and therefore apoptosis development, rather than permeabilization of the inner mitochondrial membrane (66), which would trigger an alternative non-apoptotic caspase-independent programmed cell death (67–69). The induction of SOD-2 fitted well with the kinetics of ROS generation. SOD-2 generation did not result in a decrease in overall ROS, be-

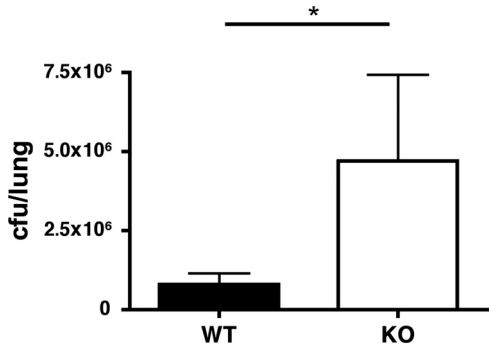

FIG. 10. **Eukaryotic elongation factor 2 (eEF2) kinase deficient mice have reduced bacterial clearance.** Bacterial counts were estimated in lungs from wild-type (WT) or eukaryotic elongation factor 2 kinase deficient (KO) mice infected with 5×10^5 colony forming units of type one *Streptococcus pneumoniae* for 24 h, $n = 11$ per group, * $p < 0.05$, Mann-Whitney *U* test. Two WT mice and one eEF2k KO mouse cleared the bacteria completely.

cause it regulates mitochondrial ROS (41) and because ROS was measured by DCF, which measures a variety of ROS species (70) but in this case it is likely to be the kind of ROS and its specific location rather than the overall quantity which influences the death program. Another of the proteins that was up-regulated in response to cathepsin D activation, HspA5, is a marker of ER stress (71). It is induced by oxidant stress and protects against certain forms of ROS-induced cell death so potentially could also dampen down the effects of excessive mitochondrial injury and necroptosis. Although HspA5 can limit induction of apoptosis in certain circumstances (71), in the context of a model with prominent apoptotic cell death, these observations suggest that cathepsin D may regulate the tension between different cell death pathways during the cell stress associated with innate immune responses in macrophages.

Interestingly, our study revealed another protein, S100A6 or calcyclin, was up-regulated in infection, but in this case pepstatin A treatment did not reverse the change but further increased up-regulation. S100A6 enhances the transcriptional activity of the tumor suppressor p53 (37) and elevated levels of S100A6 enhance apoptosis by inducing transcriptional up-regulation of caspase 3 (38). It could therefore increase the susceptibility to apoptosis after infection. It therefore might seem counter-intuitive that cathepsin D inhibition further increased S100A6 expression but cathepsin D might be acting to slow down the increase of S100A6, putting a brake on the onset of apoptosis and allowing the bactericidal function of the macrophage to continue.

Although cathepsin D inhibited competing death pathways, we found evidence that cathepsin D contributed to regulation of the mitochondrial apoptosis pathway at two key points. We have previously shown that Mcl-1 levels determine the onset of mitochondrial outer membrane permeabilization in this model (18, 72). Gelsolin regulates caspase activation (46, 47) and prevents mitochondrial outer membrane permeabilization and translocation of cytochrome *c* to the cytosol, reducing activation of caspase 9 (45). We documented that gelsolin levels declined immediately before cytochrome *c* translocation. Moreover, we also observed that cathepsin D down-regulated eEF2, which catalyzes a key translocation step during protein translation, and is therefore an important regulator of protein synthesis (73, 74). Mcl-1, which has a short half-life of only 20–30 mins is critically dependent on translation to maintain intracellular levels (50). We showed using BMDM lacking eEF2 kinase, a negative regulator of eEF2, that eEF2 activity allows maintenance of Mcl-1 expression, delays the mitochondrial apoptosis pathway and also delays apoptosis-associated macrophage killing of *S. pneumoniae*, in a murine model in which apoptosis contributes to bacterial clearance (17). eEF2 is also down-regulated following human metapneumovirus, respiratory syncytial virus, and HIV-1 infection, with increased apoptosis susceptibility (59, 75).

Modulation of protein translation via eEF2 is not a recognized point of regulation for innate host responses so this is a novel finding of our study. Microbial factors such as diphtheria toxin and the exotoxin A from *Pseudomonas aeruginosa* exploit manipulation of protein translation by targeting eEF2 for ADP-ribosylation (74), emphasizing the importance of this cell function to host responses. Protein translation is highly efficient in alveolar macrophages and maintenance of factors regulating protein translation, in their optimal phosphorylation state, is one mechanism accounting for the longevity of differentiated tissue macrophages (76). Modulation of protein translation is a potent point of regulation for macrophage commitment to apoptosis, which is manifested by alteration in molecules with very short half-lives, such as FLIP (73), or in our model Mcl-1 (18).

In conclusion, our results suggest that cathepsin D activation during host defense has multiple effects on the macrophage proteome with convergence on those pathways regulating cell death. These alterations stimulate the mitochondrial pathway of apoptosis but inhibit competing cell death pathways. This emphasizes the complexity of regulation of cell death during innate responses and emphasizes that regulation of cell death involves appropriate control of competing pathways to allow the co-ordinated induction of cell death. These results emphasize the potential of proteomics to identify novel points of regulation of death processes, as exemplified by our novel finding that regulation of protein translation is a key molecular switch controlling the commitment to apoptosis during the execution of antimicrobial host defense.

* This work is supported by a Wellcome Trust Senior Clinical Fellowship to DHD, #076945, a British Lung Foundation Fellowship to HMM, F05/7, a BBSRC grant (BB/D005469/1) to BC and from the EPSRC (EP/E036252/1) to PCW under the ChELSI initiative.

[S] This article contains supplemental Figs. S1 and S2 and Tables S1 to S4.

** To whom correspondence should be addressed: Department of Infection and Immunity, The University of Sheffield Medical School,

Beech Hill Rd, Sheffield, S10 2RX, UK. Tel: +44 (0) 114 226 1427; Fax: +44 (0) 114 226 8898; E-mail: d.h.dockrell@sheffield.ac.uk.

REFERENCES

1. Silva, M. T. When two is better than one: macrophages and neutrophils work in concert in innate immunity as complementary and cooperative partners of a myeloid phagocyte system. *J. Leuko. Biol.* **87,** 93–106
2. Shi, S., Nathan, C., Schnappinger, D., Drenkow, J., Fuortes, M., Block, E., Ding, A., Gingeras, T. R., Schoolnik, G., Akira, S., Takeda, K., and Ehrt, S. (2003) MyD88 primes macrophages for full-scale activation by interferon-gamma yet mediates few responses to Mycobacterium tuberculosis. *J. Exp. Med.* **198,** 987–997
3. Brown, J. N., Kohler, J. J., Coberley, C. R., Sleasman, J. W., and Goodenow, M. M. (2008) HIV-1 activates macrophages independent of Toll-like receptors. *PLoS One* **3,** e3664
4. Chan, G., Bivins-Smith, E. R., Smith, M. S., Smith, P. M., and Yurochko, A. D. (2008) Transcriptome analysis reveals human cytomegalovirus reprograms monocyte differentiation toward an M1 macrophage. *J. Immunol.* **181,** 698–711
5. Nares, S., Moutsopoulos, N. M., Angelov, N., Rangel, Z. G., Munson, P. J., Sinha, N., and Wahl, S. M. (2009) Rapid myeloid cell transcriptional and proteomic responses to periodontopathogenic Porphyromonas gingivalis. *Am. J. Pathol.* **174,** 1400–1414
6. Herskovits, A. A., Auerbuch, V., and Portnoy, D. A. (2007) Bacterial ligands generated in a phagosome are targets of the cytosolic innate immune system. *PLoS Pathog.* **3,** e51
7. Cohn, Z. A., and Benson, B. (1965) The differentiation of mononuclear phagocytes. morphology, cytochemistry, and biochemistry. *J. Exp. Med.* **121,** 153–170
8. Cohn, Z. A., Fedorko, M. E., and Hirsch, J. G. (1966) The in vitro differentiation of mononuclear phagocytes. V. The formation of macrophage lysosomes. *J. Exp. Med.* **123,** 757–766
9. Kato, T., Kojima, K., and Murachi, T. (1972) Proteases of macrophages in rat peritoneal exudate, with special reference to the effects of actinomycete protease inhibitors. *Biochim. Biophys. Acta.* **289,** 187–193
10. Woessner Jr., J. F. (1992) Role of cellular proteinases and their protein inhibitors in inflammation. In: Whicher, J. T., and Evans, S. W., eds. *Biochemistry of inflammation*, pp. 57–90, Kluwer Academic Publishers, Hingham
11. Sintiprungrat, K., Singhto, N., Sinchaikul, S., Chen, S. T., and Thongboonkerd, V. Alterations in cellular proteome and secretome upon differentiation from monocyte to macrophage by treatment with phorbol myristate acetate: insights into biological processes. *J. Proteomics* **73,** 602–618
12. Benes, P., Vetvicka, V., and Fusek, M. (2008) Cathepsin D–many functions of one aspartic protease. *Crit. Rev. Oncol. Hematol.* **68,** 12–28
13. Conus, S., Perozzo, R., Reinheckel, T., Peters, C., Scapozza, L., Yousefi, S., and Simon, H. U. (2008) Caspase-8 is activated by cathepsin D initiating neutrophil apoptosis during the resolution of inflammation. *J. Exp. Med.* **205,** 685–698
14. Carrasco-Marin, E., Madrazo-Toca, F., de Los Toyos, J. R., Cacho-Alonso, E., Tobes, R., Pareja, E., Paradela, A., Albar, J. P., Chen, W., Gomez-Lopez, M. T., and Alvarez-Dominguez, C. (2009) The innate immunity role of cathepsin-D is linked to Trp-491 and Trp-492 residues of listeriolysin O. *Mol. Microbiol.*
15. Bewley, M. A., Marriott, H. M., Tulone, C., Francis, S. E., Mitchell, T. J., Read, R. C., Chain, B., Kroemer, G., Whyte, M. K. B., and Dockrell, D. H. (2011) A Cardinal Role for Cathepsin D in Co-ordinating the Host-mediated Apoptosis of Macrophages and Killing of Pneumococci *PLoS Pathogens,* In Press
16. Dockrell, D. H., Lee, M., Lynch, D. H., and Read, R. C. (2001) Immune-mediated phagocytosis and killing of Streptococcus pneumoniae are associated with direct and bystander macrophage apoptosis. *J. Infect. Dis.* **184,** 713–722
17. Dockrell, D. H., Marriott, H. M., Prince, L. R., Ridger, V. C., Ince, P. G., Hellewell, P. G., and Whyte, M. K. (2003) Alveolar macrophage apoptosis contributes to pneumococcal clearance in a resolving model of pulmonary infection. *J. Immunol.* **171,** 5380–5388
18. Marriott, H. M., Bingle, C. D., Read, R. C., Braley, K. E., Kroemer, G., Hellewell, P. G., Craig, R. W., Whyte, M. K., and Dockrell, D. H. (2005) Dynamic changes in Mcl-1 expression regulate macrophage viability or commitment to apoptosis during bacterial clearance. *J. Clin. Invest.* **115,** 359–368
19. Daigneault, M., Preston, J. A., Marriott, H. M., Whyte, M. K., and Dockrell, D. H. The identification of markers of macrophage differentiation in PMA-stimulated THP-1 cells and monocyte-derived macrophages. *PLoS One* **5,** e8668
20. Tulone, C., Uchiyama, Y., Novelli, M., Grosvenor, N., Saftig, P., and Chain, B. M. (2007) Haematopoietic development and immunological function in the absence of cathepsin D. *BMC Immunol.* **8,** 22
21. Ryazanov, A. G. (2002) Elongation factor-2 kinase and its newly discovered relatives. *FEBS Lett.* **514,** 26–29
22. Gan, C. S., Chong, P. K., Pham, T. K., and Wright, P. C. (2007) Technical, experimental, and biological variations in isobaric tags for relative and absolute quantitation (iTRAQ). *J. Proteome Res.* **6,** 821–827
23. Pham, T. K., Sierocinski, P., van der Oost, J., and Wright, P. C. (2010) Quantitative proteomic analysis of Sulfolobus solfataricus membrane proteins. *J Proteome Res* **9,** 1165–1172
24. Chong, P. K., and Wright, P. C. (2005) Identification and characterization of the Sulfolobus solfataricus P2 proteome. *J. Proteome Res.* **4,** 1789–1798
25. Ow, S. Y., Salim, M., Noirel, J., Evans, C., Rehman, I., and Wright, P. C. (2009) iTRAQ underestimation in simple and complex mixtures: "the good, the bad and the ugly". *J. Proteome Res.* **8,** 5347–5355
26. Aly, T. A., Ide, A., Jahromi, M. M., Barker, J. M., Fernando, M. S., Babu, S. R., Yu, L., Miao, D., Erlich, H. A., Fain, P. R., Barriga, K. J., Norris, J. M., Rewers, M. J., and Eisenbarth, G. S. (2006) Extreme genetic risk for type 1A diabetes. *Proc. Natl. Acad. Sci. U.S.A.* **103,** 14074–14079
27. Elias, J. E., and Gygi, S. P. (2007) Target-decoy search strategy for increased confidence in large-scale protein identifications by mass spectrometry. *Nat. Methods* **4,** 207–214
28. Pham, T. K., Roy, S., Noirel, J., Douglas, I., Wright, P. C., and Stafford, G. P. (2010) A quantitative proteomic analysis of biofilm adaptation by the periodontal pathogen Tannerella forsythia. *Proteomics* **10,** 3130–3141
29. Hiraoka, W., Vazquez, N., Nieves-Neira, W., Chanock, S. J., and Pommier, Y. (1998) Role of oxygen radicals generated by NADPH oxidase in apoptosis induced in human leukemia cells. *J. Clin. Invest.* **102,** 1961–1968
30. Gordon, S. B., Irving, G. R., Lawson, R. A., Lee, M. E., and Read, R. C. (2000) Intracellular trafficking and killing of Streptococcus pneumoniae by human alveolar macrophages are influenced by opsonins. *Infect. Immun.* **68,** 2286–2293
31. Laury-Kleintop, L. D., Coronel, E. C., Lange, M. K., Tachovsky, T., Longo, S., Tucker, S., and Alhadeff, J. A. (1995) Western blotting and isoform analysis of cathepsin D from normal and malignant human breast cell lines. *Breast Cancer Res. Treat.* **35,** 211–220
32. Long, B. J., and van den Berg, H. W. (1996) Reduced levels of cathepsin D associated with tamoxifen resistance and estrogen independence in the ZR-75–1 human breast cancer cell line. *Cancer Lett.* **99,** 233–238
33. Bidère, N., Lorenzo, H. K., Carmona, S., Laforge, M., Harper, F., Dumont, C., and Senik, A. (2003) Cathepsin D triggers Bax activation, resulting in selective apoptosis-inducing factor (AIF) relocation in T lymphocytes entering the early commitment phase to apoptosis. *J. Biol. Chem.* **278,** 31401–31411
34. Deiss, L. P., Galinka, H., Berissi, H., Cohen, O., and Kimchi, A. (1996) Cathepsin D protease mediates programmed cell death induced by interferon-gamma, Fas/APO-1 and TNF-alpha. *EMBO J.* **15,** 3861–3870
35. Maclean, K. H., Dorsey, F. C., Cleveland, J. L., and Kastan, M. B. (2008) Targeting lysosomal degradation induces p53-dependent cell death and prevents cancer in mouse models of lymphomagenesis. *J. Clin. Invest.* **118,** 79–88
36. Capony, F., Morisset, M., Barrett, A. J., Capony, J. P., Broquet, P., Vignon, F., Chambon, M., Louisot, P., and Rochefort, H. (1987) Phosphorylation, glycosylation, and proteolytic activity of the 52-kD estrogen-induced protein secreted by MCF7 cells. *J. Cell Biol.* **104,** 253–262
37. Słomnicki, L. P., Nawrot, B., and Leśniak, W. (2009) S100A6 binds p53 and affects its activity. *Int. J. Biochem. Cell Biol.* **41,** 784–790
38. Joo, J. H., Yoon, S. Y., Kim, J. H., Paik, S. G., Min, S. R., Lim, J. S., Choe, I. S., Choi, I., and Kim, J. W. (2008) S100A6 (calcyclin) enhances the sensitivity to apoptosis via the upregulation of caspase-3 activity in Hep3B cells. *J. Cell. Biochem.* **103,** 1183–1197
39. Williams, M. D., Van Remmen, H., Conrad, C. C., Huang, T. T., Epstein, C. J., and Richardson, A. (1998) Increased oxidative damage is corre-

lated to altered mitochondrial function in heterozygous manganese superoxide dismutase knockout mice. *J. Biol. Chem.* **273,** 28510–28515
40. Nathan, C. (1992) Nitric oxide as a secretory product of mammalian cells. *FASEB J.* **6,** 3051–3064
41. Fridovich, I. (1999) Fundamental aspects of reactive oxygen species, or what's the matter with oxygen? *Ann. N.Y. Acad. Sci.* **893,** 13–18
42. Tchatalbachev, S., Ghai, R., Hossain, H., and Chakraborty, T. (2010) Gram-positive pathogenic bacteria induce a common early response in human monocytes. *BMC Microbiol* **10,** 275
43. Shi, L., Chowdhury, S. M., Smallwood, H. S., Yoon, H., Mottaz-Brewer, H. M., Norbeck, A. D., McDermott, J. E., Clauss, T. R., Heffron, F., Smith, R. D., and Adkins, J. N. (2009) Proteomic investigation of the time course responses of RAW 264.7 macrophages to infection with Salmonella enterica. *Infect. Immun.* **77,** 3227–3233
44. Sun, H. Q., Yamamoto, M., Mejillano, M., and Yin, H. L. (1999) Gelsolin, a multifunctional actin regulatory protein. *J. Biol. Chem.* **274,** 33179–33182
45. Koya, R. C., Fujita, H., Shimizu, S., Ohtsu, M., Takimoto, M., Tsujimoto, Y., and Kuzumaki, N. (2000) Gelsolin inhibits apoptosis by blocking mitochondrial membrane potential loss and cytochrome c release. *J. Biol. Chem.* **275,** 15343–15349
46. Ohtsu, M., Sakai, N., Fujita, H., Kashiwagi, M., Gasa, S., Shimizu, S., Eguchi, Y., Tsujimoto, Y., Sakiyama, Y., Kobayashi, K., and Kuzumaki, N. (1997) Inhibition of apoptosis by the actin-regulatory protein gelsolin. *EMBO J.* **16,** 4650–4656
47. Kamada, S., Kusano, H., Fujita, H., Ohtsu, M., Koya, R. C., Kuzumaki, N., and Tsujimoto, Y. (1998) A cloning method for caspase substrates that uses the yeast two-hybrid system: cloning of the antiapoptotic gene gelsolin. *Proc. Natl. Acad. Sci. U.S.A.* **95,** 8532–8537
48. Galluzzi, L., and Kroemer, G. (2008) Necroptosis: a specialized pathway of programmed necrosis. *Cell* **135,** 1161–1163
49. Liu, H., Perlman, H., Pagliari, L. J., and Pope, R. M. (2001) Constitutively activated Akt-1 is vital for the survival of human monocyte-differentiated macrophages. Role of Mcl-1, independent of nuclear factor (NF)-kappaB, Bad, or caspase activation. *J. Exp. Med.* **194,** 113–126
50. Schubert, K. M., and Duronio, V. (2001) Distinct roles for extracellular-signal-regulated protein kinase (ERK) mitogen-activated protein kinases and phosphatidylinositol 3-kinase in the regulation of Mcl-1 synthesis. *Biochem. J.* **356,** 473–480
51. Ryazanov, A. G., Shestakova, E. A., and Natapov, P. G. (1988) Phosphorylation of elongation factor 2 by EF-2 kinase affects rate of translation. *Nature* **334,** 170–173
52. McLeod, L. E., and Proud, C. G. (2002) ATP depletion increases phosphorylation of elongation factor eEF2 in adult cardiomyocytes independently of inhibition of mTOR signalling. *FEBS Lett.* **531,** 448–452
53. Park, S., Park, J. M., Kim, S., Kim, J. A., Shepherd, J. D., Smith-Hicks, C. L., Chowdhury, S., Kaufmann, W., Kuhl, D., Ryazanov, A. G., Huganir, R. L., Linden, D. J., and Worley, P. F. (2008) Elongation factor 2 and fragile X mental retardation protein control the dynamic translation of Arc/Arg3.1 essential for mGluR-LTD. *Neuron* **59,** 70–83
54. Schwacke, J. H., Hill, E. G., Krug, E. L., Comte-Walters, S., and Schey, K. L. (2009) iQuantitator: a tool for protein expression inference using iTRAQ. *BMC Bioinformatics* **10,** 342
55. Hill, E. G., Schwacke, J. H., Comte-Walters, S., Slate, E. H., Oberg, A. L., Eckel-Passow, J. E., Therneau, T. M., and Schey, K. L. (2008) A statistical model for iTRAQ data analysis. *J. Proteome Res.* **7,** 3091–3101
56. Ow, S. Y., Noirel, J., Salim, M., Evans, C., Watson, R., and Wright, P. C. Balancing robust quantification and identification for iTRAQ: application of UHR-ToF MS. *Proteomics* **10,** 2205–2213
57. Goldmann, O., von Köckritz-Blickwede, M., Höltje, C., Chhatwal, G. S., Geffers, R., and Medina, E. (2007) Transcriptome analysis of murine macrophages in response to infection with Streptococcus pyogenes reveals an unusual activation program. *Infect. Immun.* **75,** 4148–4157
58. Rogers, P. D., Thornton, J., Barker, K. S., McDaniel, D. O., Sacks, G. S., Swiatlo, E., and McDaniel, L. S. (2003) Pneumolysin-dependent and -independent gene expression identified by cDNA microarray analysis of THP-1 human mononuclear cells stimulated by Streptococcus pneumoniae. *Infect. Immun.* **71,** 2087–2094
59. van Diepen, A., Brand, H. K., Sama, I., Lambooy, L. H., van den Heuvel, L. P., van der Well, L., Huynen, M., Osterhaus, A. D., Andeweg, A. C., and Hermans, P. W. (2010) Quantitative proteome profiling of respiratory virus-infected lung epithelial cells. *J. Proteomics*
60. Ohman, T., Rintahaka, J., Kalkkinen, N., Matikainen, S., and Nyman, T. A. (2009) Actin and RIG-I/MAVS signaling components translocate to mitochondria upon influenza A virus infection of human primary macrophages. *J. Immunol.* **182,** 5682–5692
61. Ferguson, J. B., Andrews, J. R., Voynick, I. M., and Fruton, J. S. (1973) The specificity of cathepsin D. *J. Biol. Chem.* **248,** 6701–6708
62. Mahrus, S., Trinidad, J. C., Barkan, D. T., Sali, A., Burlingame, A. L., and Wells, J. A. (2008) Global sequencing of proteolytic cleavage sites in apoptosis by specific labeling of protein N termini. *Cell* **134,** 866–876
63. Marriott, H. M., Jackson, L. E., Wilkinson, T. S., Simpson, A. J., Mitchell, T. J., Buttle, D. J., Cross, S. S., Ince, P. G., Hellewell, P. G., Whyte, M. K., and Dockrell, D. H. (2008) Reactive oxygen species regulate neutrophil recruitment and survival in pneumococcal pneumonia. *Am. J. Respir. Crit. Care Med.* **177,** 887–895
64. Gorman, A., McGowan, A., and Cotter, T. G. (1997) Role of peroxide and superoxide anion during tumour cell apoptosis. *FEBS Lett.* **404,** 27–33
65. Clement, M. V., Ponton, A., and Pervaiz, S. (1998) Apoptosis induced by hydrogen peroxide is mediated by decreased superoxide anion concentration and reduction of intracellular milieu. *FEBS Lett.* **440,** 13–18
66. Madesh, M., and Hajnóczky, G. (2001) VDAC-dependent permeabilization of the outer mitochondrial membrane by superoxide induces rapid and massive cytochrome c release. *J. Cell Biol.* **155,** 1003–1015
67. Leist, M., and Nicotera, P. (1997) The shape of cell death. *Biochem. Biophys. Res. Commun.* **236,** 1–9
68. Yu, L., Wan, F., Dutta, S., Welsh, S., Liu, Z., Freundt, E., Baehrecke, E. H., and Lenardo, M. (2006) Autophagic programmed cell death by selective catalase degradation. *Proc. Natl. Acad. Sci. U.S.A.* **103,** 4952–4957
69. Xu, Y., Kim, S. O., Li, Y., and Han, J. (2006) Autophagy contributes to caspase-independent macrophage cell death. *J. Biol. Chem.* **281,** 19179–19187
70. Hempel, S. L., Buettner, G. R., O'Malley, Y. Q., Wessels, D. A., and Flaherty, D. M. (1999) Dihydrofluorescein diacetate is superior for detecting intracellular oxidants: comparison with 2′,7′-dichlorodihydrofluorescein diacetate, 5(and 6)-carboxy-2′,7′-dichlorodihydrofluorescein diacetate, and dihydrorhodamine 123. *Free Radic. Biol. Med.* **27,** 146–159
71. Rao, R. V., Ellerby, H. M., and Bredesen, D. E. (2004) Coupling endoplasmic reticulum stress to the cell death program. *Cell Death Differ.* **11,** 372–380
72. Marriott, H. M., Ali, F., Read, R. C., Mitchell, T. J., Whyte, M. K., and Dockrell, D. H. (2004) Nitric oxide levels regulate macrophage commitment to apoptosis or necrosis during pneumococcal infection. *FASEB J.* **18,** 1126–1128
73. Davies, C. C., Mason, J., Wakelam, M. J., Young, L. S., and Eliopoulos, A. G. (2004) Inhibition of phosphatidylinositol 3-kinase- and ERK MAPK-regulated protein synthesis reveals the pro-apoptotic properties of CD40 ligation in carcinoma cells. *J. Biol. Chem.* **279,** 1010–1019
74. Jørgensen, R., Merrill, A. R., and Andersen, G. R. (2006) The life and death of translation elongation factor 2. *Biochem. Soc. Trans.* **34,** 1–6
75. Zelivianski, S., Liang, D., Chen, M., Mirkin, B. L., and Zhao, R. Y. (2006) Suppressive effect of elongation factor 2 on apoptosis induced by HIV-1 viral protein R. *Apoptosis* **11,** 377–388
76. Monick, M. M., Powers, L. S., Gross, T. J., Flaherty, D. M., Barrett, C. W., and Hunninghake, G. W. (2006) Active ERK contributes to protein translation by preventing JNK-dependent inhibition of protein phosphatase 1. *J. Immunol.* **177,** 1636–1645